

Electrical Wind Force-Driven and Dislocation-Templated Amorphization in Phase-Change Materials

Sung-Wook Nam^{1*}, Ju Li^{1,2}, and Ritesh Agarwal¹

¹ Department of Materials Science and Engineering, University of Pennsylvania, Philadelphia, PA 19104, USA

² Department of Nuclear Science and Engineering and Department of Materials Science and Engineering, Massachusetts Institute of Technology, Cambridge, MA 02139, USA

*Current address: IBM T.J. Watson Research Center, Yorktown Heights, NY 10598, USA, e-mail: nams@us.ibm.com

ABSTRACT

We report electrical wind force-driven behaviors in phase-change materials, in both cases of applying DC voltage bias and AC voltage pulse. In the first part of the paper, we discuss electrical field-induced mass transport behaviors when DC voltage bias is applied in a line shape Ge₂Sb₂Te₅ (GST) device. We identified a mass transport behavior under 3~4 MA/cm² current density which raises the temperature up to ~300 °C by joule heating, implying that the mass transport of GST occurs in hexagonal phase (solid state) regime. In the second part of the paper, we report *in situ* transmission electron microscopy (TEM) observation of crystalline-to-amorphous phase transition when electrical voltage pulses are applied. The voltage pulses produce dislocations in GST, by generating vacancies through thermal heat shock process followed by condensing the vacancies in a rapid cooling process. By the electrical wind force, the dislocations become mobile and glide in the direction of hole-carrier motion. Directional motions of dislocations induce a jamming at the certain location, which eventually leads amorphization switching. Our investigations suggest that the crystalline-to-amorphous phase-transition of GST might be a solid-state process.

Key words: *in situ* TEM, phase-change nanowire, wind force, dislocation, mass transport, elemental separation

1. INTRODUCTION

Phase change materials have rapid electrical switching behaviors between crystalline and amorphous phases [1-3]. Understanding of the effect of electrical voltage bias is important for designing fast and low power phase-change memory devices. In the first part of the paper, we discuss electrical field-induced mass transport behaviors in the case of applying DC voltage bias in line shape GST devices [4]. Continuous voltage bias induced a mass transport by separating two different regions: mass-accumulated and mass-depleted regions. This experiment validates the presence of electrical wind force in GST, when DC voltage bias is applied with 3~4 MA/cm² current density. Based on the verifications of the electrical wind force, we extended its implications by exploring electrical switching behaviors.

In the second part of the paper, we report *in situ* TEM observations of electrical switching behaviors in GST nanowire device, in the case of applying electrical voltage pulses (AC voltage bias) [5]. Electrical wind force is deeply engaged in the electrical switching behaviors by introducing one dimensional defect structure, namely “dislocation”. In our observation, electrical voltage pulses populated dislocations in GST by condensing vacancies through thermal heat-shock process followed by rapid cooling process. The dislocation plays a catalytic role, especially in crystalline-to-amorphous phase transition. In particular, as the dislocations feel the electrical wind force, they become mobile in the direction of hole-carrier motion and collect other defect structures spreading in GST materials. Density functional theory (DFT) calculation shows that basal (0001)[11-20] slip system in GST provides a favorable pathway of the motion of prismatic dislocation loops. The directional motions of dislocations induce a catastrophic jamming which eventually leads amorphization behavior.

2. EXPERIMENTS

For the experiment of applying DC voltage bias, we fabricated GST line shape device by using sputtered GST film (100 nm thickness). E-beam lithography and reactive ion etching (RIE) processes were employed for device fabrication. The GST line shape structures were connected by Ti/Au electrode patterned by liftoff process. The contact region is far from the GST thin line shape structure, thus free from the effect of electrode contact between GST and metal materials. For electrical characterization, we used parameter analyzer (4156C, Agilent) to apply DC voltage bias and read the electrical current.

For the experiment of *in situ* TEM observations, we deigned GST nanowire device on silicon nitride (SiN) membrane. For electrical connections, SiN membrane was aligned with Ti/Au metal-line structures patterned by

photolithography and liftoff process. Upon the SiN membrane, we drilled trench structures by focus ion beam (FIB). The trench structures on the membrane are void structures where TEM electron beam is completely transparent. GST nanowires were grown by vapor-liquid-solid (VLS) method [6]. The nanowires were transferred on the SiN membrane structure, and connected by Pt deposition by FIB. After equipping the GST nanowire device in *in situ* TEM holder, Au wire was connected between the GST nanowire device and the feed-through of the TEM holder. Pulse generator, power supply and switching box were controlled by labview software. We used JEOL-2010F TEM (200 keV) for imaging the GST nanowire device.

3. RESULTS & DISCUSSIONS

- Presence of Electrical Wind Force: DC Voltage Bias Sweeping Experiments

We investigated a fundamental material property of GST material by applying continuous DC electrical bias [4]. Line shape GST device was designed in which line width (w), line length (l) and film thickness (t) are $w=1\ \mu\text{m}$, $l=5\ \mu\text{m}$, and $t=100\ \text{nm}$. External DC voltage bias was applied from 0 to 25 V by voltage sweeping, and electric current was characterized. Since we used DC voltage bias for the experiment, electrical switching behaviors (such as SET or RESET) could not be expected. Rather, this experiment was designed to understand the intrinsic material response as continuous external voltage bias.

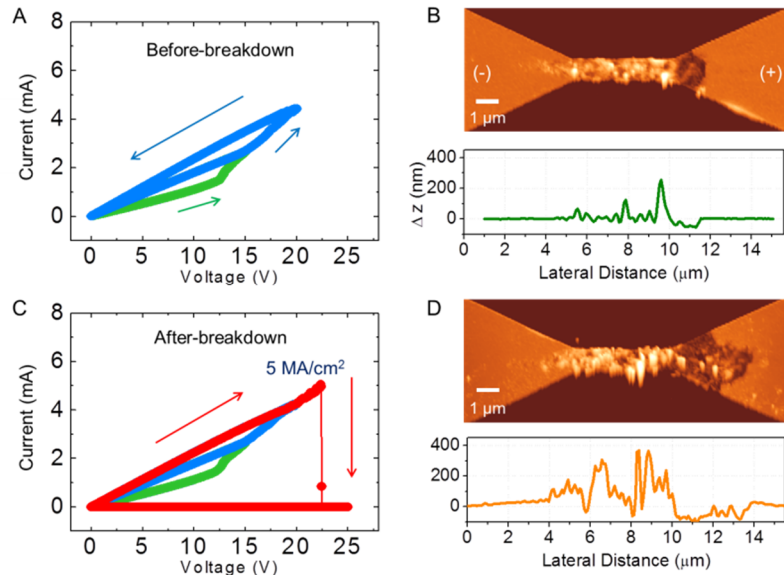


Figure 1. Correlation of DC voltage bias sweeping with microstructural evolution. (A) I-V curve of 0 to 20 V sweeping. After 0 to 20 V sweeping, the device is still electrically-connected. (B) Atomic force microscope (AFM) image of the 0 to 20 V sweeping sample (before-breakdown). The center of line has surface extrusion, while the entrance of line facing (+) electrode has surface erosion. (C) I-V curve of 0 to 25 V sweeping. The device suffers from permanent breakdown. (D) AFM image of the 0 to 25 V sweeping sample (after-breakdown).

We prepared two sample devices: one was under 0 to 20 V sweeping, and the other was under 0 to 25 V sweeping. As shown in I-V curves in Figure 1a and 1c, voltage bias sweeping of 0 to 20 V left the device still electrically-connected, while 0 to 25 V sweeping induced a permanent breakdown. From now, we call the device of 0 to 20 V sweeping as “before-breakdown sample”, while the device of 0 to 25 V sweeping as “after-breakdown sample”. One interesting aspect is that the microstructure was modified asymmetrically depending on the polarity of voltage bias. The structural modification of the line shape device was observable even through optical microscope, implying that the influence of external voltage bias on microstructural evolution was very significant in a wide range of area of the line shape device [4]. Details of the tendencies of structural evolution were investigated by atomic force microscopy (AFM). Figure 1b and 1d show AFM images of the line shape devices that experienced voltage bias sweeping of 0 to 20 V and 0 to 25 V, respectively. In both samples, the surface morphology was evolved in asymmetrical manner, by dividing two separate regions: the line center has surface extrusion while the line entrance facing (+) electrode has surface erosion. Note that the asymmetrical evolution was identified even before breakdown (0 to 20 V sweeping) in Fig. 1b. It implies that the surface morphology evolution by voltage bias is not a result of device failure but an intrinsic material property of GST.

For the GST line devices, the increase of temperature by joule heating was calculated through finite element analysis method, as shown in figure 2. In the calculations, the voltage bias of 15~20 V raises the temperature of the device to $\sim 300\ ^\circ\text{C}$ which corresponds to the temperature of hexagonal phase of GST. It implies that the mass transport behavior of GST takes place as the form of solid state. Also note that, at 15~20 V, the current density was 3~4 MA/cm² which is even less than RESET current density, such as $\sim 40\ \text{MA/cm}^2$. [7]. Our observation has two implications: (1) In

GST, external voltage bias induces a mass transport from (+) electrode to (-) electrode by electrical wind force. Since GST has p-type character [3], the mass transport behavior is supposed to be pronounced in the direction of hole-carrier motion [8]. (2) In our estimation of the increase of temperature by joule heating, the mass transport behavior is an event of solid state, rather than liquid state.

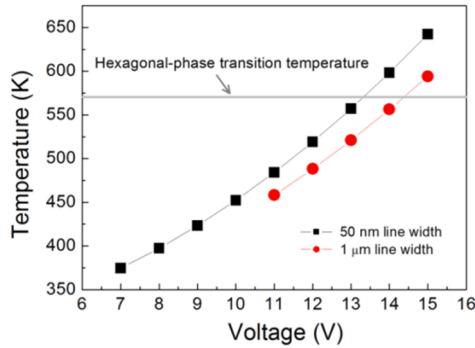


Figure 2. Calculation of the temperature by joule heating in GST line device: The horizontal line corresponds to 300 °C (573 K) which is cubic-to-hexagonal transition temperature. In our observation, the mass transport was initiated at 15~20 V. At this voltage regime, the temperature was calculated as just above 300 °C, implying that the mass transport behavior takes place as a form of solid state phase.

- Elemental Separation by Voltage Bias

For two samples of 0 to 20 V (before-breakdown) and 0 to 25 V sweeping (after-breakdown), we characterized scanning Auger spectroscopy to investigate spatial distribution of chemical compositions. Auger spectroscopy is capable of characterizing elemental variations with high surface-sensitivity. We characterized elemental mapping of Ge, Sb and Te, for the line shape devices, as shown in Figure 3a-3c. For the before-breakdown sample, we could not identify any significant contrast in elemental mapping images (not shown in this report), in spite of the pronounced mass transport behaviors with surface structural modification. However, for the after-breakdown sample, the elemental separation was identified especially at the mass depleted region where electrical breakdown was most likely to happen due to physical weakness. In the breakdown region, elemental separation takes places such that Sb-rich region is towards (-) electrode while Te-rich region is towards (+) electrode, as shown in Figure 3d.

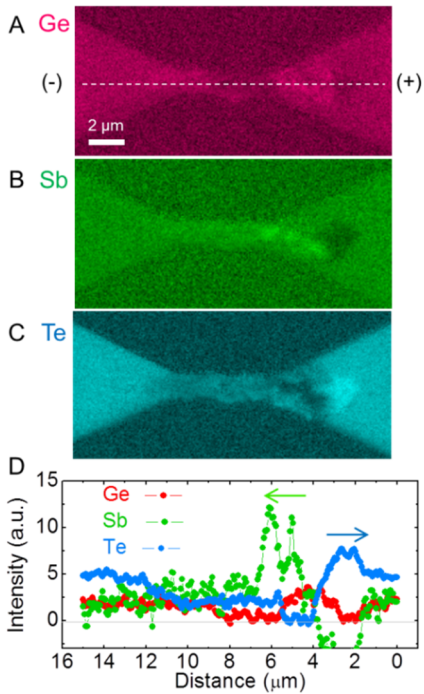


Figure 3. Scanning Auger spectroscopy for after-breakdown sample (0 to 25 V sweeping): Elemental mapping of (A) Ge, (B) Sb, and (C) Te. Line scanning shows that the elemental separation was pronounced at the mass-depleted region where electrical breakdown was supposed to happen, such that Sb-rich region is located towards (-) electrode while Te-rich region towards (+) electrode.

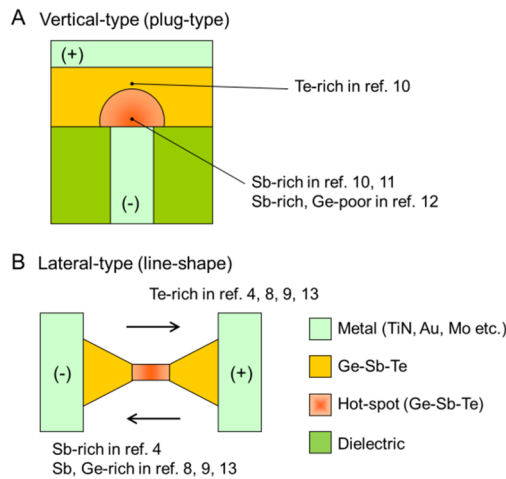


Figure 4. Tendencies of elemental separations of GST device in (A) plug-type devices and (B) lateral-type line shape devices: Depending on the bias polarity, Te-rich phase is located towards (+) electrode, while Ge, Sb-rich phase towards (-) electrode. [4, 8-13]

Considering electronegativity of Ge, Sb and Te elements, Sb and Te elements are most likely to behave as (+) and (-) ions, respectively [9]. During electrical breakdown process, the disconnecting region might severely suffer from joule heating and shape distortion, thus enabling electric current to be highly localized at the moment of electrical breakdown. The disconnecting region, where elemental separation was pronounced, was possibly to experience a melt

state (liquid state). In our experiments, the mass transport and the elemental separation behaviors were observed in different voltage bias regimes: the mass transport was initiated as a solid state phase before electrical breakdown (0 to 20 V), while the elemental separation was identified during breakdown (0 to 25 V) at higher temperature by joule heating. Figure 4 summarizes the tendency of elemental separation behaviors of GST, along with those reported from other research groups [4, 8-13]. It consistently reveals that Ge and Sb atoms move towards (-) electrode whereas Te atom moves towards (+) electrode, implying that the electrostatic forces are applied on each atoms depending on their own characters. Interestingly, total mass turns out to move towards (-) electrode, which shows that hole-carrier wind force is regarded as another dominant driving force of atomic migration, thinking of p-type electrical character of GST. Therefore, we think that the elemental separation behavior is substantially along with the mass transport behavior. Even if the elemental separation was not identified during solid-state mass transport behavior in our observation, the elemental separation is possibly to be pronounced as the results of repeated applications of voltage bias in solid-state. In fact, the elemental separation behavior in solid state has been reported in electrical stress biasing experiment [8].

- Dislocation-Templated Amorphization of GST: Applying Voltage Pulses (AC Voltage Bias)

We investigate electrical switching behavior of GST line device as applying electrical voltage pulses [5]. Electrical wind force, identified in the experiments using DC voltage bias, is assumed to influence the electrical switching behavior of GST material. To correlate structural evolutions with the applied voltage pulses, we designed *in situ* transmission electron microscope (TEM) experiments in which a GST nanowire device is electrically operated within TEM column (Figure 5a). Single crystalline structure of GST nanowire is highly beneficial, since it is free from grain boundary, thus enabling us to visualize dynamics of defect structures in a single grain structure.

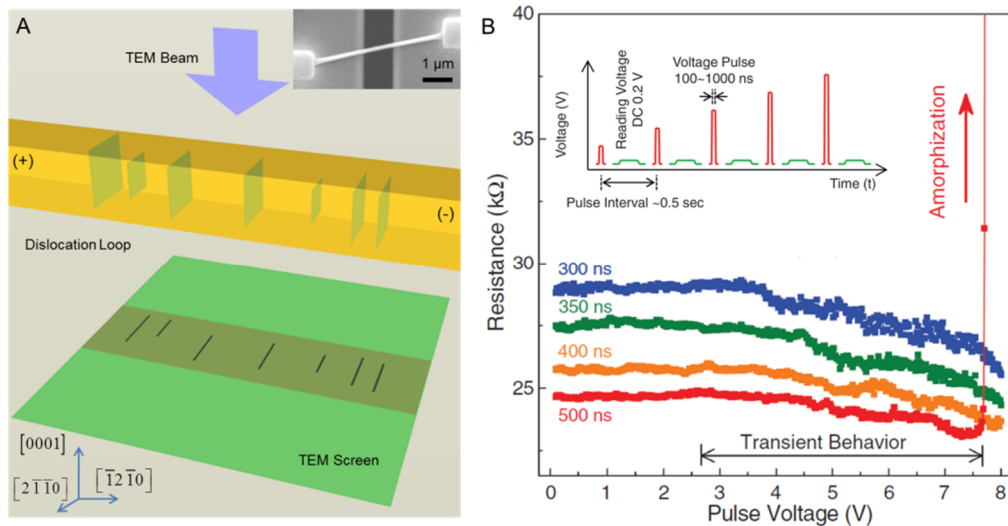


Figure 5. (A) Schematic of *in situ* TEM experiments using GST nanowire device. (Inset) Scanning electron microscope (SEM) image of free standing GST nanowire crossing trench region. (B) A plot of electrical resistance versus the amplitude of voltage pulses. Notably, the resistance was slightly decreased (resistance-dip; transient behavior) before amorphization switching. (Inset) Sequence of electrical pulses applied to the nanowire device.

For TEM imaging of the electrical switching behaviors, we correlated the electrical resistance variations with dark-field (DF) TEM images which are more sensitive for imaging defect structures. The electrical resistance was measured between each voltage pulse with ~0.5 s pulse-interval. Note that the electrical resistance decreases slightly just before amorphization switching, as shown in Figure 5b. The decrease of electrical resistance (resistance-dip) was correlated with dynamic contrast changes in DF TEM images in Figure 6b to 6f, which implies that the motions of line-shaped defect structures (dislocations) are deeply engaged in crystalline-to-amorphous phase transition. Upon approaching the bottom of the resistance-dip, the dislocations stopped moving (jamming), followed by the formation of highly accumulated and entangled dislocations at the jammed location, in Figure 6g and 6h. Finally, the electrical resistance was increased by two orders of magnitude (electrical switching), which is correlated with a generation of a bright line amorphous structure (indicated by red arrow) in Figure 6i.

In our investigations, the electrical voltage pulse plays two important roles: One is to populate dislocations by vacancy condensation through thermal heat shock process followed by rapid cooling, and the other is to transport dislocations by electrical wind force in the direction of hole-carrier which is the majority carrier of GST. This transient behavior before amorphization switching implies that the entangled dislocations are precursors for amorphization switching process.

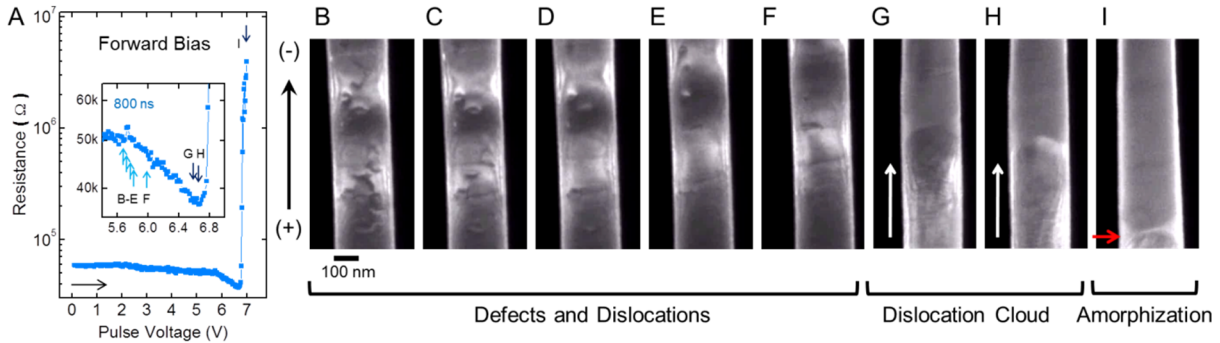


Figure 6. *In situ* TEM observation of the crystalline-to-amorphous phase transition by applying electrical voltage pulses. (A) Plot of electrical resistance versus voltage pulse amplitude. (B-I) The resistance-dip is correlated with DF TEM. Voltage pulses created dislocations and transported them in the direction of hole-carrier motion in B to F. At the bottom of the resistance-dip, a dislocation cloud was observed in G and H. Amorphization occurred at the jammed region (red-arrow) in I.

To define the phase-change region, we sculpted a notch structure which has a role of geometrical constriction. We identified that highly entangled dislocation-cloud is accumulated behind the notch, at the transient of crystalline-to-amorphous phase transition (in Figure 7).

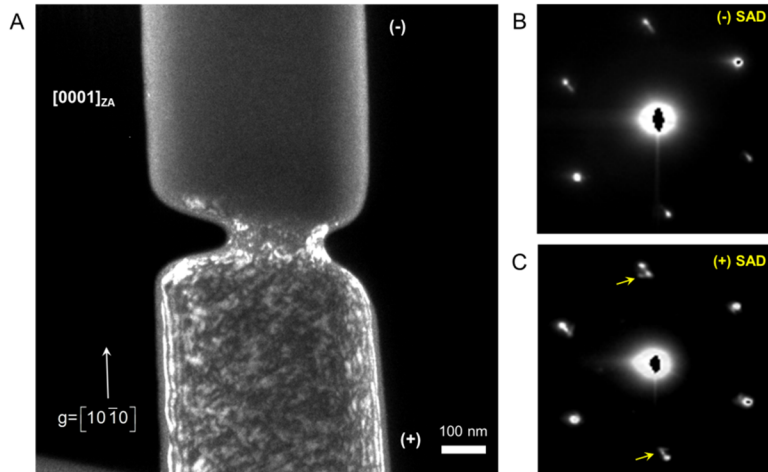


Figure 7. DF TEM image of notch-shaped GST nanowire device at the transient of crystalline-to-amorphous phase transition: (A) A dislocation cloud was located behind the notch where dislocation jamming occurred by geometrical constriction. (B,C) Selected area diffraction (SAD) patterns in (-) and (+) electrode regions. In (+) electrode region where dislocation cloud was located, an elongation of diffraction spot (yellow arrows) was identified. The elongation of diffraction spot implies lattice distortion by defect structures.

We suggest a model for the crystalline-to-amorphous phase transition by incorporating dislocation dynamics, as shown in figure 8. Density functional theory (DFT) calculation [14] shows that, in GST, basal (0001)[11-20] slip system has extremely low generalized stacking fault (GSF) energy, such as 10.1 mJ/m² in figure 8a. This GSF energy value of GST (10.1 mJ/m²) is very small compared with Cu (169 mJ/m²) or Silicon (>1500 mJ/m²) [14]. Such a low GSF energy of GST is attributed to the layered structures with a stacking sequence -Sb-Te-Ge-Te-Te-Ge-Te-Sb-Te- [15]. In particular, weak bonding nature of Te-Te layers on the basal plane provides a pathway of the motion of prismatic dislocation loops driven by the electrical wind force.

We summarize the dislocation generation and dynamics leading to amorphization switching in Figure 8b. Electrical voltage pulses nucleate dislocations by vacancy condensation through thermal heat shock followed by rapid cooling process. As voltage pulse amplitude is increased, the dislocations feel electrical wind force thus becoming mobile and gliding in the direction of hole-carrier motion. During dislocation transport, the dislocations collect other defect structures spreading GST material, thus lowering the electrical resistance (resistance-dip). The mobile dislocations are accumulated and jammed at certain location, which eventually leads to amorphization switching behavior.

4. CONCLUSION

In this paper, we report electrical wind force-driven behaviors in phase-change materials. By using both DC and AC voltage bias, we have explored fundamental material properties, such as mass transport behavior and dislocation-templated amorphization behavior. Our investigations show that electrical wind force plays a unique role in rapid switching behaviors of GST, by generating and transporting dislocations. The presence of electrical wind force and the

capability of generating and transporting dislocations might be one of the reasons of the rapid electrical switching behavior of phase-change materials.

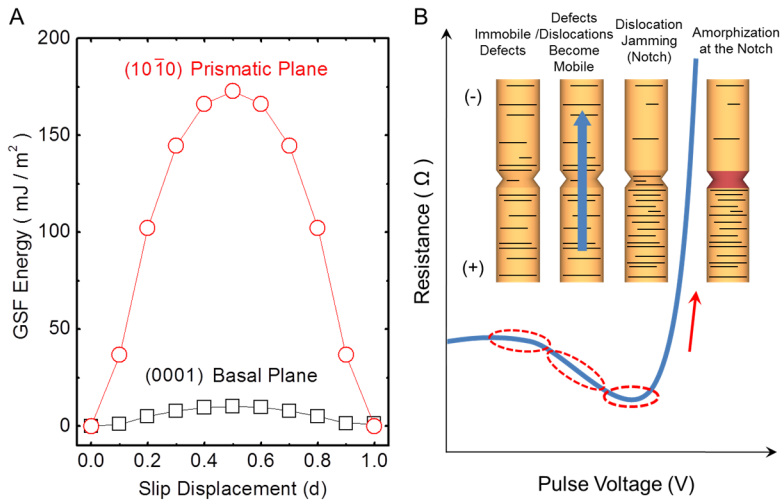


Figure 8. (A) DFT calculation of GSF energy for prismatic and basal slip systems of GST. Low GSF energy in (0001) basal plane of GST offers a favorable pathway of the motion of prismatic dislocation loops. (B) Our model about (1) dislocation generation, (2) transport, (3) jamming followed by (4) amorphization. Electrical voltage pulses generate dislocations by vacancy condensation through thermal heat shock process followed by rapid cooling. Dislocations feel electrical wind force, thus becoming mobile and gliding. Mobile dislocation collects defect structures, thus lowering the electrical resistance (resistance-dip), which induces a jamming at certain location. The jammed dislocations finally lead amorphization.

REFERENCES

- [1] A. V. Kolobov et al., *Nat. Mater.* **3**, 703 (2004).
- [2] M. Wuttig, N. Yamada, *Nat. Mater.* **6**, 824 (2007).
- [3] S. Raoux, *Annu. Rev. Mater. Res.* **39**, 25 (2009).
- [4] S. W. Nam et al., *Electrochem. Solid-State Lett.* **12**, H155 (2009).
- [5] S. W. Nam et al., *Science* **336**, 1561 (2012).
- [6] S. H. Lee, Y. Jung, R. Agarwal, *Nat. Nanotechnol.* **2**, 626 (2007).
- [7] H. S. P. Wong et al., *Proceedings of the IEEE* **98**, 2201 (2010).
- [8] T. Y. Yang, I. M. Park, B. J. Kim, Y. C. Joo, *Appl. Phys. Lett.* **95**, 032104 (2009).
- [9] D. Kang et al., *Appl. Phys. Lett.* **95**, 011904 (2009).
- [10] J. B. Park et al., *J. Electrochem. Soc.* **154**, H139 (2007).
- [11] S. M. Yoon et al., *Appl. Surf. Sci.* **254**, 316 (2007).
- [12] S. Raoux et al., *Microelectron. Eng.* **85**, 2330 (2008).
- [13] C. Kim et al., *Appl. Phys. Lett.* **94**, 193504 (2009).
- [14] S. Ogata, J. Li, S. Yip, *Phys. Rev. B* **71**, 224102 (2005).
- [15] Z. M. Sun, J. Zhou, R. Ahuja, *Phys. Rev. Lett.* **96**, 055507 (2006).

Biographies

Sung-Wook Nam completed his doctorate (Ph.D) in Materials Science in Seoul National University in 2009. He studied phase-change nonvolatile-memory devices and nanopore/nanochannel ionic transistors. While he was a graduate student, he has visited IBM Watson Research Center for one year (2007-2008). After obtaining Ph.D, he joined in University of Pennsylvania as postdoctoral researcher (2009-2011). He studied in situ TEM observations of electrical switching behaviors in nanowire phase-change memory devices. Now, he is working in IBM Watson Research Center as research scientist. He has published 20 peer-reviewed papers.

Ju Li is Battelle Energy Alliance Professor of Nuclear Science and Engineering and a Full Professor of Materials Science and Engineering at MIT. Using atomistic modeling and in situ experiments, his group (<http://li.mit.edu>) investigates mechanical, electrochemical and transport behaviours of materials, often under extreme stress, temperature and radiation environments. Ju obtained a Ph.D. degree in nuclear engineering from MIT in 2000, and Bachelor's degree in Physics from University of Science and Technology of China in 1994. He is a winner of the 2005 Presidential Early Career Award for Scientists and Engineers, 2006 MRS Outstanding Young Investigator Award, and 2007 TR35 award from the Technology Review magazine.

Ritesh Agarwal earned his undergraduate degree from the Indian Institute of Technology, Kanpur in 1996, and a master's degree in chemistry from the University of Chicago. He received his PhD in physical chemistry from the University of California at Berkeley in 2001. After completing his PhD., Ritesh was a postdoctoral fellow at Harvard where he studied the optical and photonic properties of semiconductor nanowires. His work led to the development of electrically-driven single nanowire lasers and avalanche photodiodes. Ritesh is currently an associate professor in the Department of Materials Science and Engineering at the University of Pennsylvania. His research interests include optics and electronics in nanowires, and studying phase transitions and electronic memory switching at the nanoscale. Ritesh is the recipient of the NSF CAREER award in 2007 and the NIH Director's New Innovator Award in 2010.